Electronic supplementary Information (ESI †) for

Electrochemical Oxidation of Boron-Doped Nickel-Iron Layered Double Hydroxide for Facile Charge Transfer in Oxygen Evolution Electrocatalysts

In-Kyoung Ahn[a], So-Yeon Lee[a], Hyoung Gyun Kim[a], Gi-Baek Lee[a], Ji-Hoon Lee[b], Miyoung Kim[a], and Young-Chang Joo*[,a,c,d]

[a]*Department of Materials Science & Engineering, Seoul National University, Seoul 08826, Republic of Korea*

[b]*Materials Center for Energy Convergence, Surface Technology Division, Korea Institute of Materials Science (KIMS), Changwon, Gyeongnam 51508, Republic of Korea*

[c]*Research Institute of Advanced Materials (RIAM), Seoul National University, Seoul 08826, Republic of Korea*

[d]*Advanced Institute of Convergence Technology, 145 Gwanggyo-ro, Yeongtong-gu, Suwon 16229, Republic of Korea*

***Corresponding authors:**
Young-Chang Joo
E-mail: ycjoo@snu.ac.kr, Tel: +82-2-880-8986, Fax: +82-2-883-8197

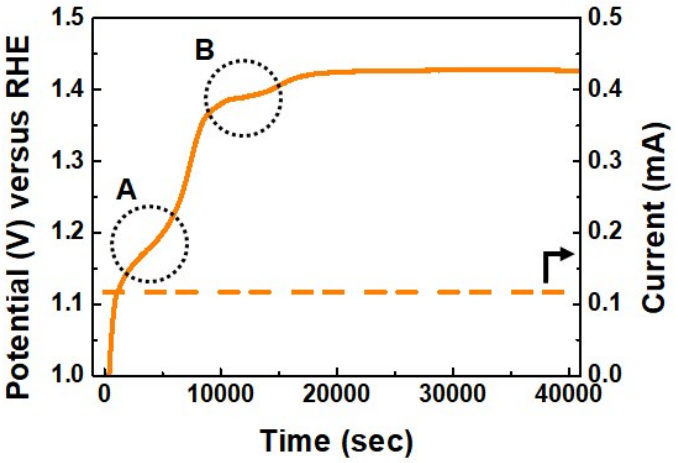

A: $M^{2+} \rightarrow M^{3+} + e^-$ (M: Ni, Fe, etc.)

B: $M^{3+} + 2H_2O + 3OH^- \rightarrow$ **M-OOH** $+ 3H_2O$

Fig. S1 The potential profile of the galox-B:NiFe LDH during galvanostatic oxidation at 0.1 mA cm^{-2} over 12 hours. Observation of two plateaus during oxidation[S18].

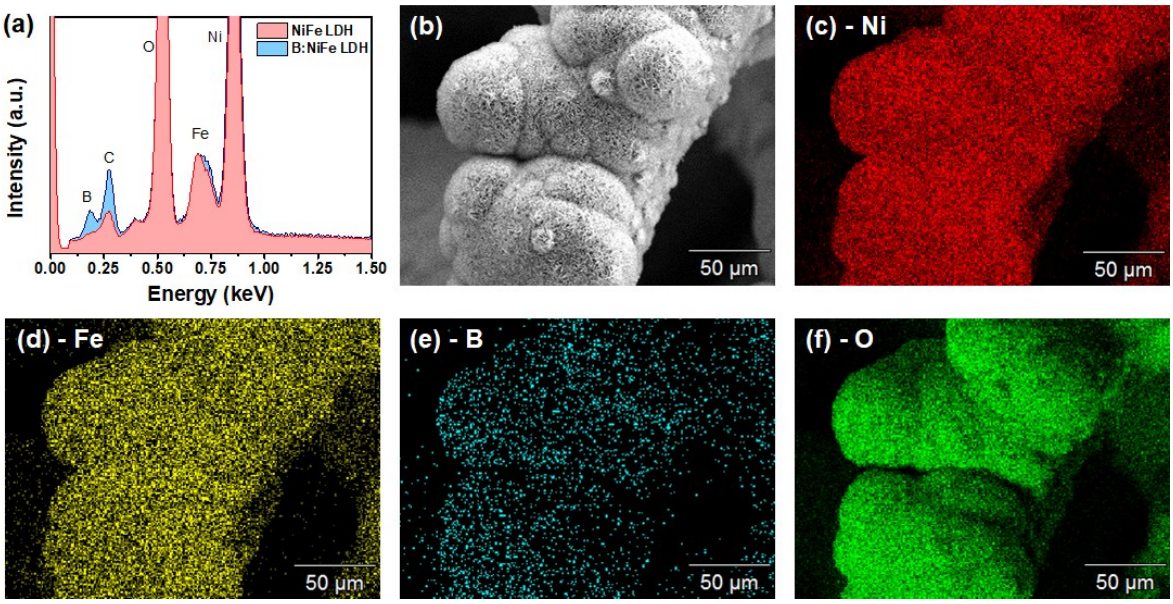

Fig. S2 Morphological characterization of B:NiFe LDH. (a) Energy dispersive X-ray spectrometry (EDS) spectrum. (b) EDS scanning image. (c-f) EDS elemental mapping images of B:NiFe LDH. (c) Ni. (d) Fe. (e) B, (f) O.

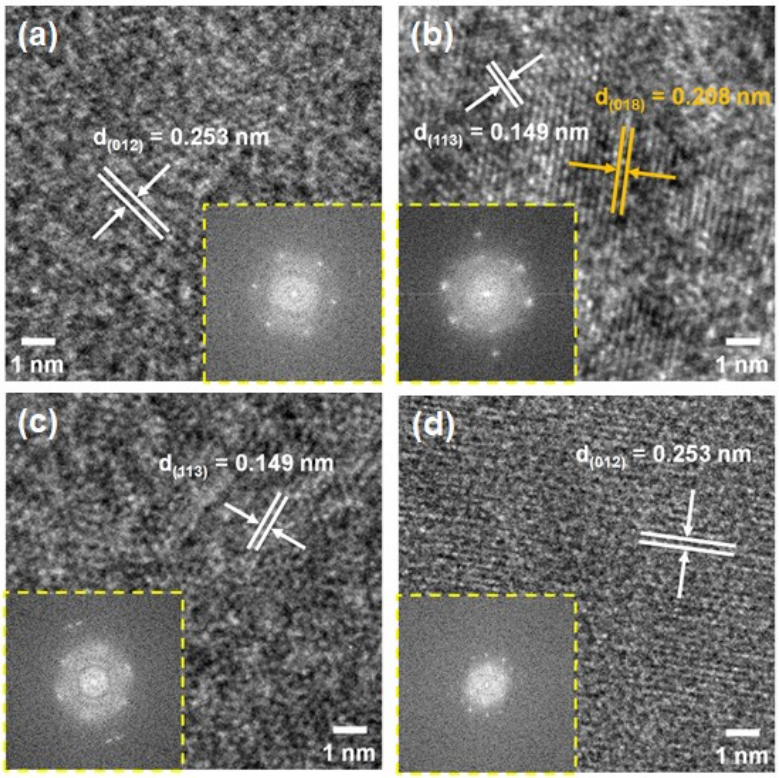

Fig. S3 Microstructural characterization of NiFe LDH based electrocatalysts. HR-TEM and FFT analysis (inset) of (a) NiFe LDH, (b) B:NiFe LDH, (c) B:NiFe LDH after OER sweep, and (d) galox-B:NiFe LDH.

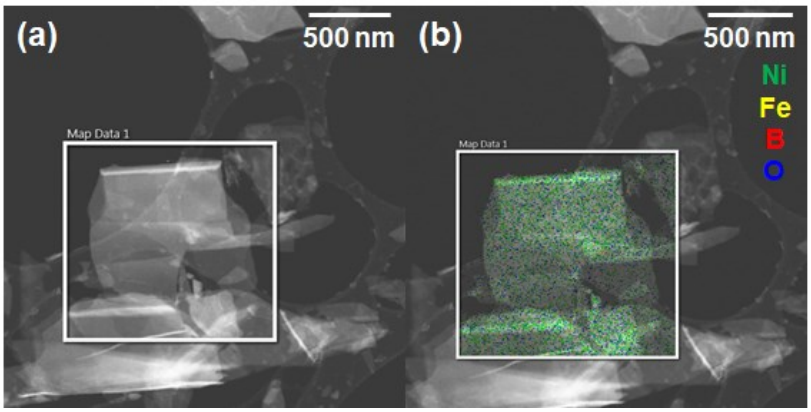

Fig. S4 EDS of TEM analysis of B:NiFe LDH. (a) STEM image. (b) Mixed EDS layered image of STEM, Ni, Fe, B, and O composition.

Table S1. ICP-AES analysis for verification of chemical composition of NiFe LDH base electrocatalysts

Sample	Ni (ppm)	B (ppm)	Ni : B ratio
NiFe LDH	7.5×10^3	0	**1 : 0**
B:NiFe LDH	7.9×10^3	18.8	**1 : 0.013**
Galox-B:NiFe LDH	9.0×10^3	0.25	**$1 : 0.1 \times 10^{-3}$**

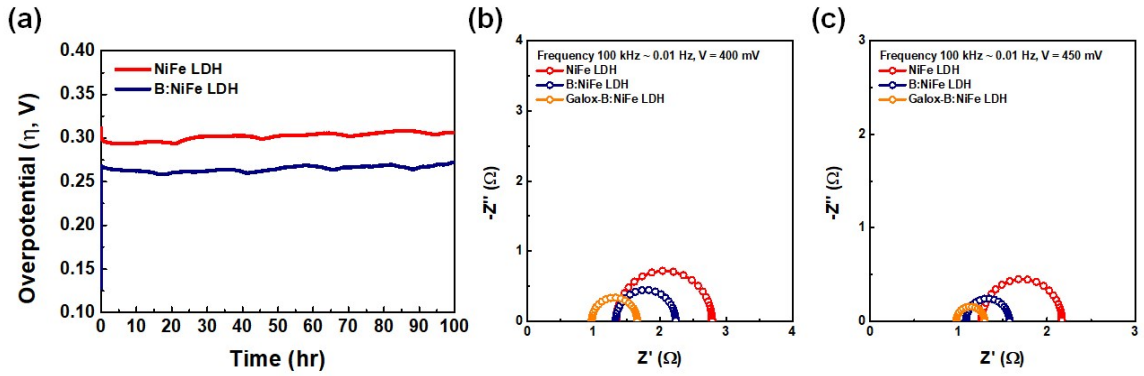

Fig. S5 Electrochemical characterization of NiFe LDH based electrocatalysts in 1.0 M KOH. (a) Chronopotentiometric stability test of NiFe LDH and B:NiFe LDH at constant current density 10 mA cm^{-2}. Nyquist plots at (b) 400 mV (vs. RHE) and (c) 450 mV (vs. RHE) for different electrodes.

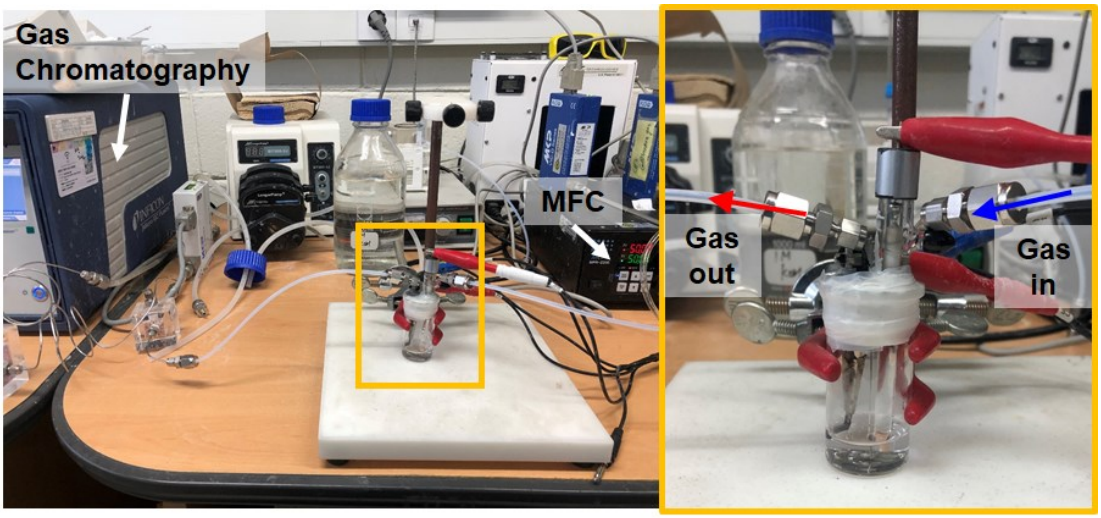

$$FE\ (\%) = \frac{Z \cdot n \cdot F}{Q}$$

Z: number of electrons for 1 mol gas

n: number of moles

F: Faraday constant, 96,500 C mol^{-1}

Q: passed charge

$$2H_2O + 2e^- \rightarrow H_2 + 2OH^-$$

$$4OH^- \rightarrow 2H_2O + O_2 + 4e^-$$

Fig. S6 Images of equipment of evolved gas analysis during stability test. The equation of bottom of images: calculation of Faradaic efficiency.

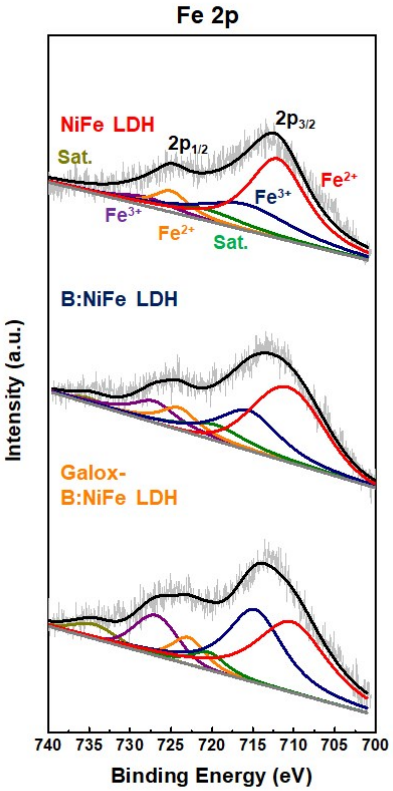

Fig. S7 XPS analysis for observation of Fe 2p of NiFe LDH based electrocatalysts under each condition.

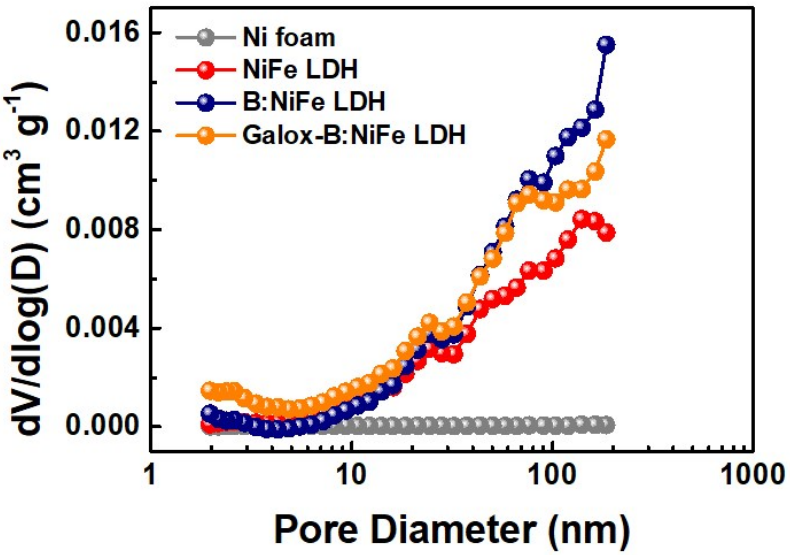

Fig. S8 Physically porosity characterization of pore diameter distribution of NiFe LDH based electrocatalysts.

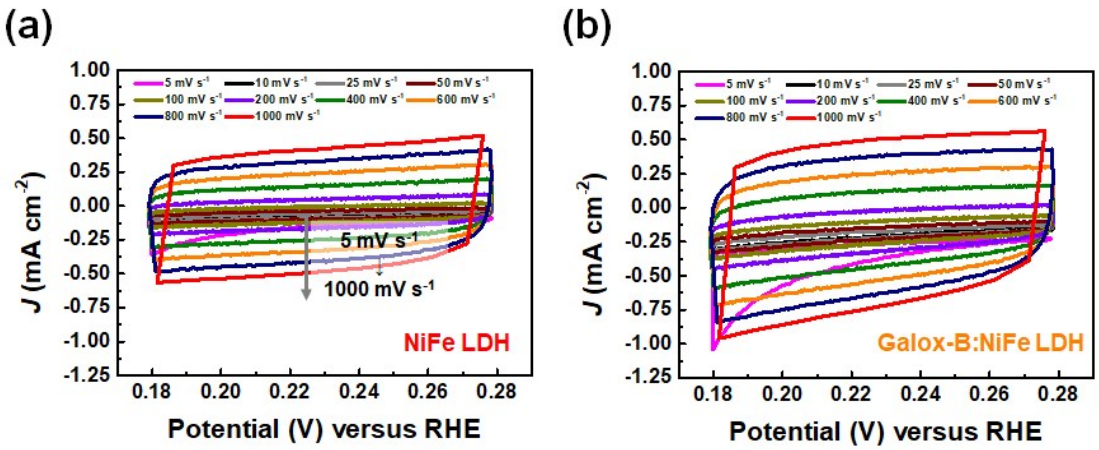

Fig. S9 Cyclic voltammogram for measurement of ECSA of (a) NiFe LDH and (b) galox-B:NiFe LDH.

The cyclic voltammetry (CV) was performed in the voltage range between 0.18 and 0.28 V (vs. RHE, non-Faradaic range). The linear slope was calculated by plotting ΔJ at 0.23 V (vs. RHE) depending on scan rates. The double-layer capacitance (C_{dl}) was calculated through the 1/2 of linear slope value[S1,S2,S4,S6].

$\Delta J = J_a - J_c$, C_{dl} can be calculated following equation:

$C_{dl} = 1/2 \times d(\Delta J)/dv$

The ECSA can be calculated following equation[S3-S6]:

ECSA = C_{dl}/C_s, C_s: The capacitance of atomically smooth planar surface in 1.0 M KOH electrolyte ranges between 20 to 60 μF cm^{-2} [S3-S5]. For calculation, C_s was configured at 40 μF cm^{-2} [S3,S5].

Electrocatalysts	Slope	C_{dl}	ECSA
NiFe LDH on Ni foam	0.9 mF cm^{-2}	0.45 mF cm^{-2}	11.25 cm^2 $_{ECSA}$
Galox-B:NiFe LDH on Ni foam	1.3 mF cm^{-2}	0.65 mF cm^{-2}	16.25 cm^2 $_{ECSA}$

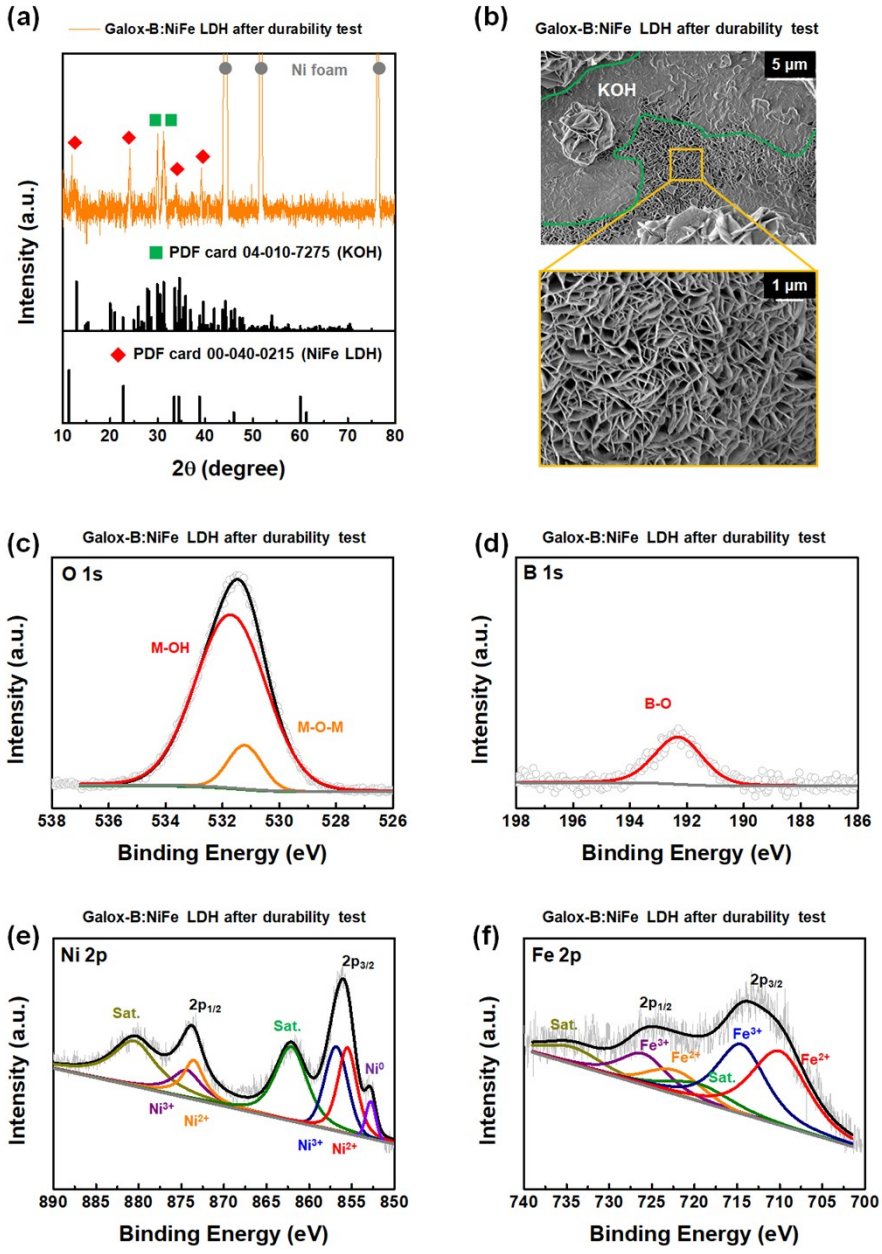

Fig. S10 Structural, morphological, and chemical characterization of galox-B:NiFe LDH electrode after OER stability test. (a) XRD analysis for observation of phase of galox-B:NiFe LDH after 100 hours OER stability test. (b) FE-SEM image of low magnification (top) and high magnification (bottom) of the galox-B:NiFe LDH. (c-f) XPS analysis. (c) oxygen 1s, (d) boron 1s, (e) nickel 2p, and (f) iron 2p spectrum.

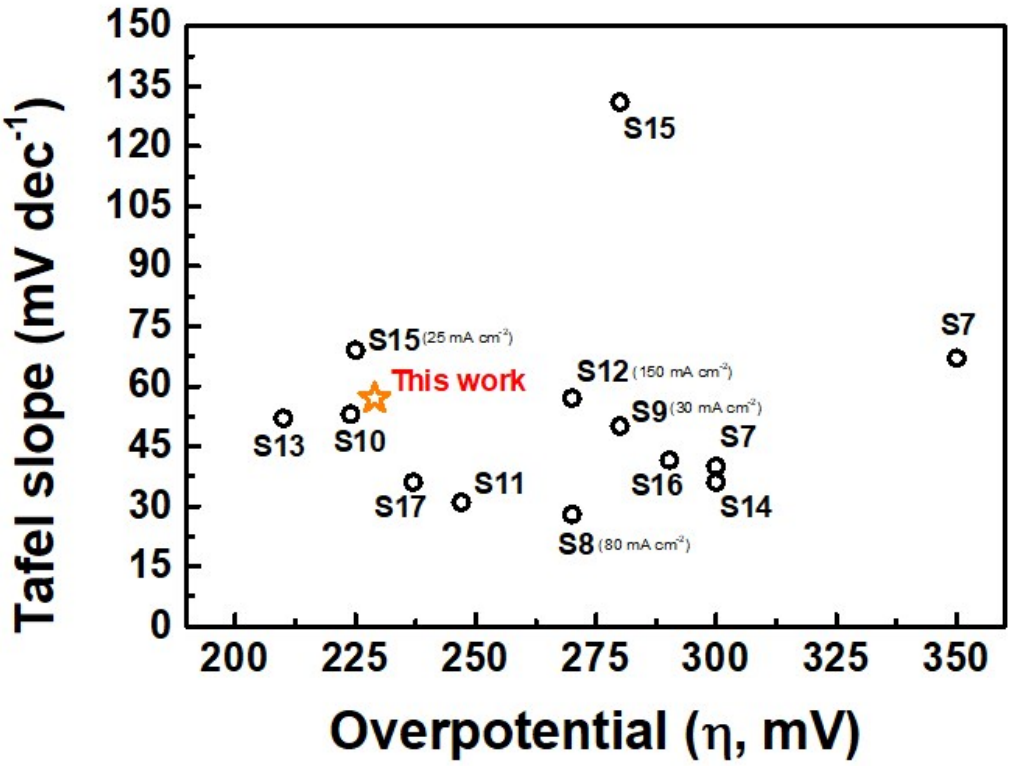

Fig. S11 Comparison of OER electrocatalytic activity at 10 mA cm^{-2} with previous reports of transition metal LDH based electrocatalysts (X-axis: overpotential, Y-axis: Tafel slope).

References

S1. Xu, X.; Song, F.; Hu, X., A nickel iron diselenide-derived efficient oxygen-evolution catalyst. *Nat Commun* **2016,** *7*, 12324.

S2. Deng, H.; Zhang, C.; Xie, Y.; Tumlin, T.; Giri, L.; Karna, S. P.; Lin, J., Laser induced MoS2/carbon hybrids for hydrogen evolution reaction catalysts. *Journal of Materials Chemistry A* **2016,** *4* (18), 6824-6830.

S3. Wang, D.; Wang, J.; Luo, X.; Wu, Z.; Ye, L., In Situ Preparation of Mo2C Nanoparticles Embedded in Ketjenblack Carbon as Highly Efficient Electrocatalysts for Hydrogen Evolution. *ACS Sustainable Chemistry & Engineering* **2017,** *6* (1), 983-990.

S4. Benck, J. D.; Chen, Z.; Kuritzky, L. Y.; Forman, A. J.; Jaramillo, T. F., Amorphous Molybdenum Sulfide Catalysts for Electrochemical Hydrogen Production: Insights into the Origin of their Catalytic Activity. *ACS Catalysis* **2012,** *2* (9), 1916-1923.

S5. McCrory, C. C.; Jung, S.; Ferrer, I. M.; Chatman, S. M.; Peters, J. C.; Jaramillo, T. F., Benchmarking hydrogen evolving reaction and oxygen evolving reaction electrocatalysts for solar water splitting devices. *J Am Chem Soc* **2015,** *137* (13), 4347-57.

S6. Ahn, I. K.; Joo, W.; Lee, J. H.; Kim, H. G.; Lee, S. Y.; Jung, Y.; Kim, J. Y.; Lee, G. B.; Kim, M.; Joo, Y. C., Metal-organic Framework-driven Porous Cobalt Disulfide Nanoparticles Fabricated by Gaseous Sulfurization as Bifunctional Electrocatalysts for Overall Water Splitting. *Sci Rep* **2019,** *9* (1), 19539.

S7. Song, F.; Hu, X., Exfoliation of layered double hydroxides for enhanced oxygen evolution catalysis. *Nat Commun* **2014,** *5*, 4477.

S8. Lu, X.; Zhao, C., Electrodeposition of hierarchically structured three-dimensional nickel-iron electrodes for efficient oxygen evolution at high current densities. *Nat Commun* **2015,** *6*, 6616.

S9. Lu, Z.; Xu, W.; Zhu, W.; Yang, Q.; Lei, X.; Liu, J.; Li, Y.; Sun, X.; Duan, X., Three-dimensional NiFe layered double hydroxide film for high-efficiency oxygen evolution reaction. *Chem Commun (Camb)* **2014,** *50* (49), 6479-82.

S10. Li, Z.; Shao, M.; An, H.; Wang, Z.; Xu, S.; Wei, M.; Evans, D. G.; Duan, X., Fast electrosynthesis of Fe-containing layered double hydroxide arrays toward highly efficient electrocatalytic oxidation reactions. *Chem Sci* **2015,** *6* (11), 6624-6631.

S11. Gong, M.; Li, Y.; Wang, H.; Liang, Y.; Wu, J. Z.; Zhou, J.; Wang, J.; Regier, T.; Wei, F.; Dai, H., An advanced Ni-Fe layered double hydroxide electrocatalyst for water oxidation.

J Am Chem Soc **2013,** *135* (23), 8452-5.

S12. Hou, Y.; Lohe, M. R.; Zhang, J.; Liu, S.; Zhuang, X.; Feng, X., Vertically oriented cobalt selenide/NiFe layered-double-hydroxide nanosheets supported on exfoliated graphene foil: an efficient 3D electrode for overall water splitting. *Energy & Environmental Science* **2016,** *9* (2), 478-483.

S13. Jia, Y.; Zhang, L.; Gao, G.; Chen, H.; Wang, B.; Zhou, J.; Soo, M. T.; Hong, M.; Yan, X.; Qian, G.; Zou, J.; Du, A.; Yao, X., A Heterostructure Coupling of Exfoliated Ni-Fe Hydroxide Nanosheet and Defective Graphene as a Bifunctional Electrocatalyst for Overall Water Splitting. *Adv Mater* **2017,** *29* (17).

S14. Dang, L.; Liang, H.; Zhuo, J.; Lamb, B. K.; Sheng, H.; Yang, Y.; Jin, S., Direct Synthesis and Anion Exchange of Noncarbonate-Intercalated NiFe-Layered Double Hydroxides and the Influence on Electrocatalysis. *Chemistry of Materials* **2018,** *30* (13), 4321-4330.

S15. Yang, Y.; Dang, L.; Shearer, M. J.; Sheng, H.; Li, W.; Chen, J.; Xiao, P.; Zhang, Y.; Hamers, R. J.; Jin, S., Highly Active Trimetallic NiFeCr Layered Double Hydroxide Electrocatalysts for Oxygen Evolution Reaction. *Advanced Energy Materials* **2018,** *8* (15), 1703189.

S16. Xue, X.; Yu, F.; Peng, B.; Wang, G.; Lv, Y.; Chen, L.; Yao, Y.; Dai, B.; Shi, Y.; Guo, X., One-step synthesis of nickel–iron layered double hydroxides with tungstate acid anions via flash nano-precipitation for the oxygen evolution reaction. *Sustainable Energy & Fuels* **2019,** *3* (1), 237-244.

S17. Zhang, J.; Liu, J.; Xi, L.; Yu, Y.; Chen, N.; Sun, S.; Wang, W.; Lange, K. M.; Zhang, B., Single-Atom Au/NiFe Layered Double Hydroxide Electrocatalyst: Probing the Origin of Activity for Oxygen Evolution Reaction. *J Am Chem Soc* **2018,** *140* (11), 3876-3879.

S18. Lee, J.-H.; Yang, T.-Y.; Kang, H.-Y.; Nam, D.-H.; Kim, N.-R.; Lee, Y.-Y.; Lee, S.-H.; Joo, Y.-C., Designing thermal and electrochemical oxidation processes for δ-MnO2 nanofibers for high-performance electrochemical capacitors. *Journal of Materials Chemistry A* 2014, 2 (20), 7197-7204.